

Supplementary Information

**Template-Assisted Colloidal Self-Assembly of
Macroscopic Magnetic Metasurfaces**

Martin Mayer^a, Moritz Tebbe^b, Christian Kuttner^{a,c}, Max J. Schnepf^a,
Tobias A.F. König^{*,a,c}, Andreas Fery^{*,a,c,d}

^aLeibniz-Institut für Polymerforschung Dresden e.V., Institute of Physical Chemistry and
Polymer Physics, Hohe Str. 6, 01069 Dresden, Germany

^bDepartment of Physical Chemistry II, University of Bayreuth, Universitätsstr. 30, 95440
Bayreuth, Germany

^cCluster of Excellence Centre for Advancing Electronics Dresden (cfaed), Technische
Universität Dresden, 01062 Dresden, Germany

^dDepartment of Physical Chemistry of Polymeric Materials, Technische Universität
Dresden, Hohe Str. 6, 01069 Dresden, Germany

*Corresponding e-mail: koenig@ipfdd.de and fery@ipfdd.de

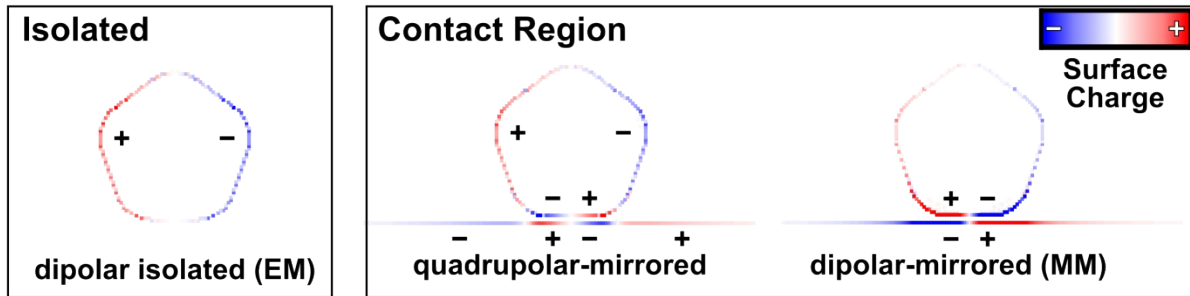


Figure S1. Surface charge plots of the isolated dipolar mode (**EM**) and the two emerging modes in the contact region. Contrary to the quadrupolar-mirrored mode at higher energies, the dipolar-mirrored mode (**MM**) induces a confinement of the charges in the contact area.

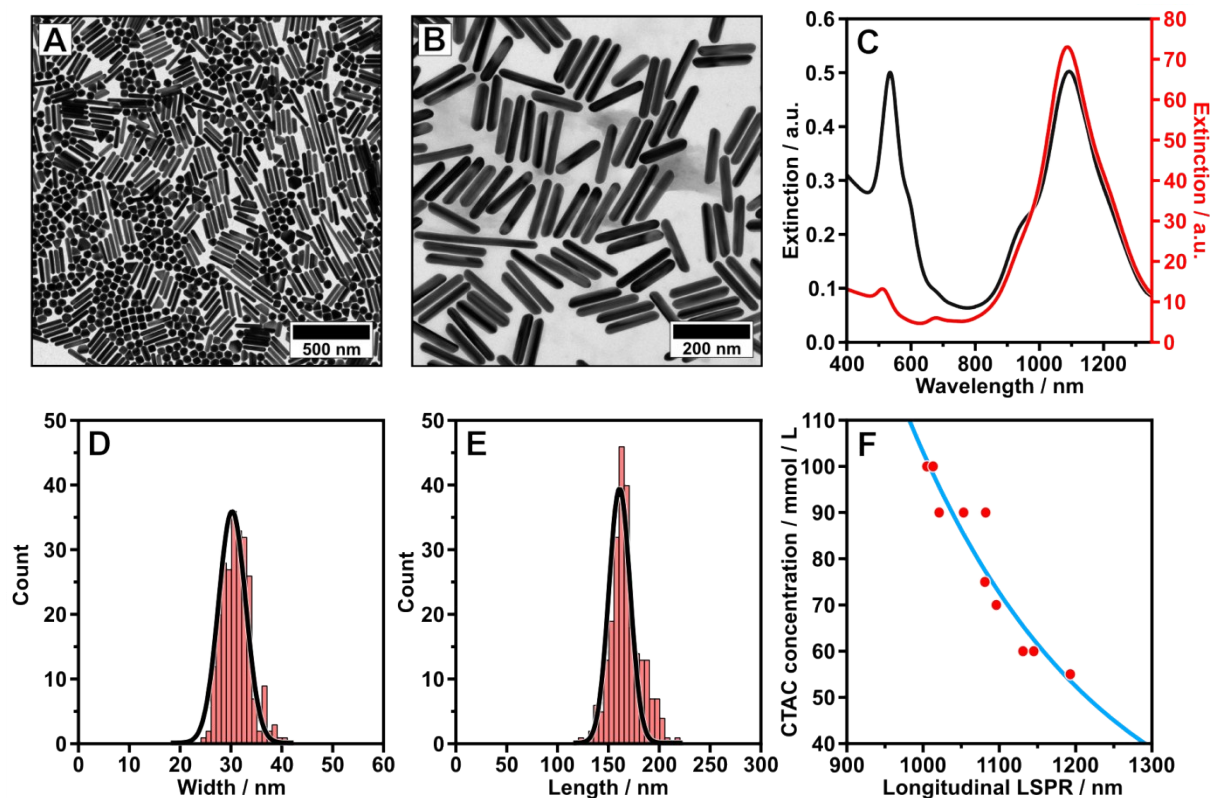


Figure S2. TEM image of the as-synthesized (A) and of the purified (B) penta-twinned gold nanorod solution. (C) Respective UV-vis-NIR spectra. Histogram plot of the evaluation of the width (D) and length (E) ($N > 250$): 161.0 ± 14.8 nm in $\langle \text{length} \rangle$ and 30.2 ± 3.7 nm in $\langle \text{width} \rangle$. (F) Calibration plot for the required CTAC concentration to purify gold nanorods depending on their longitudinal plasmon resonance. The empirical fit (blue) can be used to assign an appropriate surfactant concentration without the need of TEM study or concentration screening. For in detail explanations of the purification process please see Reference 1.¹

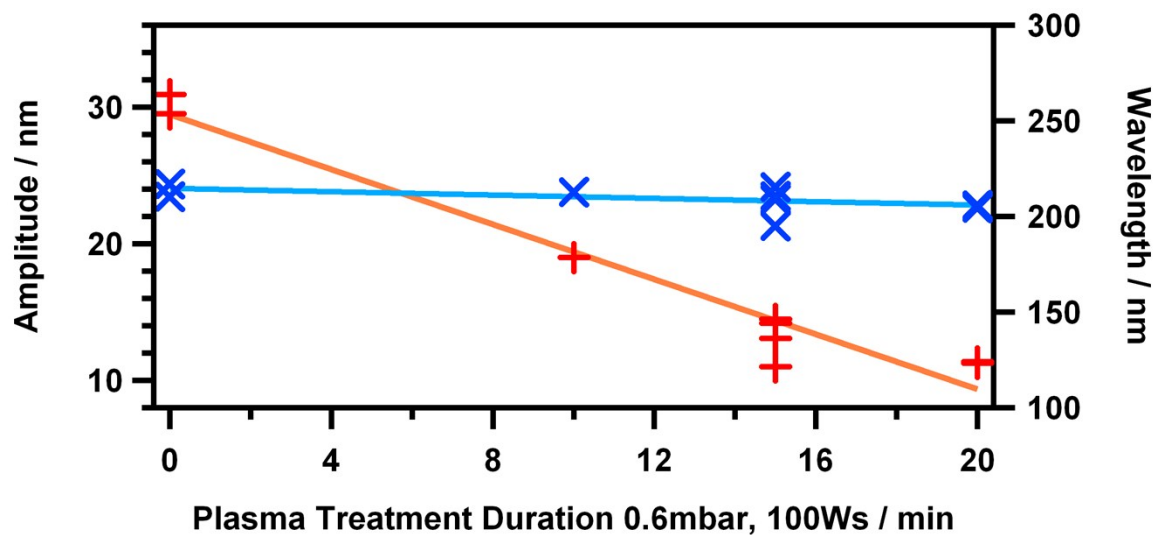


Figure S3. To match the template dimensions to the nanorod dimension for the template-assisted self-assembly process, the amplitude of the wrinkled substrate needs to be reduced by an additional plasma treatment. The amplitude (**red**) is reduced linearly with plasma dose, while the wavelength (**blue**) remains constant.

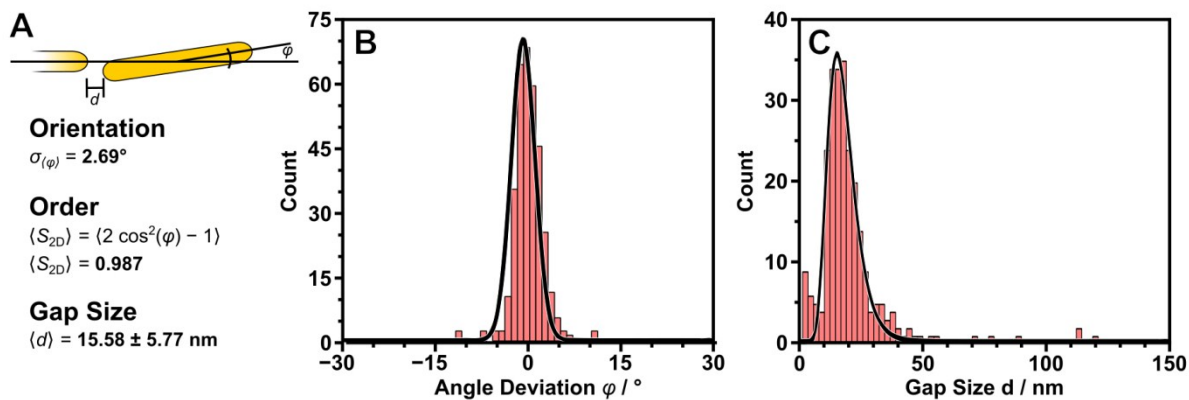


Figure S4. (A) Schematic depiction of the evaluated angle of deviation and gap size. The evaluation of over 360 individual nanorods reveals a standard deviation of the angle of 2.69° , resulting in a 2D order parameter of 0.987. The mean gap size in line is $15.6 \pm 5.8 \text{ nm}$. Histogram plots of the angle of deviation (B) and gap size (C).

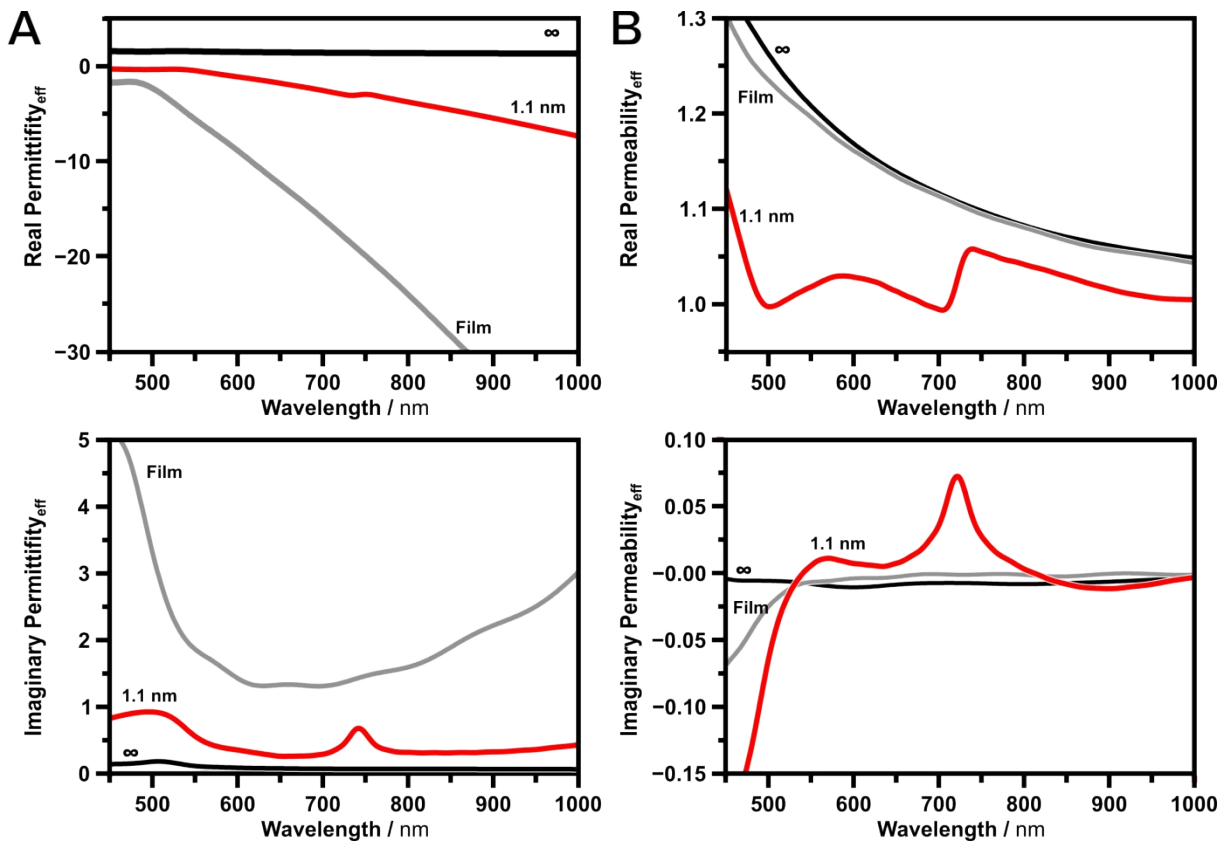


Figure S5. Calculated effective electric permittivity (**A**) and effective magnetic permeability (**B**) for a gold nanorod monomer (infinite separation from gold film, **black**), gold film only (**grey**) and film coupled nanorod at a distance of 1.1 nm (**red**).

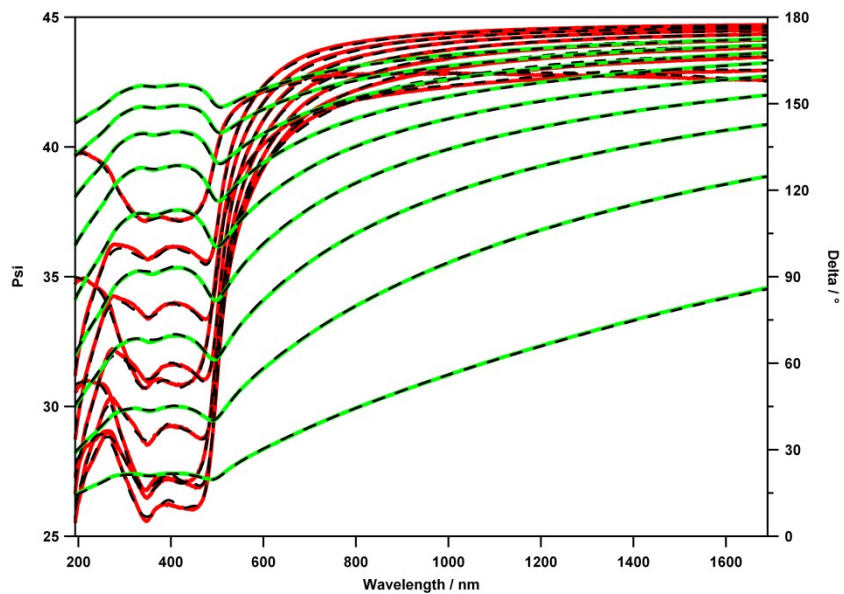


Figure S6. Variable angle spectroscopic ellipsometric data for a template-stripped gold substrate at incident angles of 45° to 85° in 5° steps. Psi (**green**) and Delta (**red**) measured in the wavelength range from 193 nm to 1690 nm. The data was fitted using a layered isotropic model of air, gold film (Cauchy), and glass substrate (Cauchy). See fit parameters in **Table S1**.

Table S1 Fitting parameter of the spectroscopic ellipsometric data measurement of the gold film on a glass substrate.

Parameter	Value	Error Bar
MSE	2.459	-
Gold Film		
Roughness / nm	0.48	0.005
Thickness / nm	34.19	0.019
Cauchy Substrate / Glass Substrate		
n @ 632 nm	1.48292	-
A	1.136	0.0049
B	0.13879	0.001510
C	0.00000	0.00011245
k Amplitude	0.32224	0.006351
Exponent	0.784	0.0064

Reference

1. M. Mayer, L. Scarabelli, K. March, T. Altantzis, M. Tebbe, M. Kociak, S. Bals, F. J. García de Abajo, A. Fery and L. M. Liz-Marzán, *Nano Lett.*, 2015, **15**, 5427-5437.